STRAIN EVOLUTION AND DAMAGE DEVELOPMENT DURING TIGHT-RADIUS BENDING OF ADVANCED HIGH STRENGTH STEELS

Nizia Mendes-Fonseca[1]* and David Wilkinson[1]

[1]*McMaster University, Hamilton, ON, Canada*
** Presenting Author email: mendesfn@mcmaster.ca*

Abstract
Improved vehicle fuel efficiency and driving safety requirements have promoted the development of Advanced High Strength Steels (AHSS) in the last few decades. The mechanical performance of AHSS is commonly characterized by the product of the ultimate tensile stress and total elongation. However, tensile elongation is not suitable for predicting the performance of a material under complex forming operations. This work aims to investigate the effect of the steel microstructure on bending performance and to make a parallel between strain partitioning and damage nucleation in tension and bending.

1. Introduction

Advanced High Strength Steels (AHSS) are recognized for their excellent tradeoff between uniform tensile elongation and strength, as extensively reported in the well-known banana diagram. However, the ductility measured using uniform elongation fails to predict damage initiation during local forming operations required to fabricate complex automotive parts, which involve tight-radius bending and edge stretching [1]. The role of the microstructure of AHSS on strain partitioning and damage development during uniaxial tensile loading has been comprehensively assessed [2-4]. But research on different stress states and strain paths is still in its early stages [5, 6]. Therefore, it is crucial to understand how the microstructure of AHSS affects their behavior in tension and tight-radius bending.

This work investigates a dual phase (DP) and a quench and partition (QP) steel with a nominal strength of 980 MPa under tensile and bend loading at the macro and microscales. The strain evolution at the macroscale was evaluated through conventional tensile and V-bend testing coupled with Digital Image Correlation (DIC). The strain partitioning between the microstructural constituents was assessed by quasi in situ SEM tensile and bend testing combined with DIC. X-ray computed tomography was employed to quantitatively measure the three-dimensional damage development with applied strain for both loading conditions.

2. Results

The main experimental results are summarized below:

a) Fractography shows that both materials fail by different mechanisms under bending and tension.
b) In situ SEM tests reveal that strain is partitioned between the steel constituents with ferrite, the softer phase in both steels, accommodating more deformation than the others (Fig.1).
c) Damage nucleates mainly by decohesion of the interface between a soft and hard phase and due to cracking of martensite islands. The strain gradient at the interface drives decohesion.
d) Damage nucleation and growth are delayed in the QP980 steel.

3. Conclusions

Ductile fracture during tight-radius bending occurs by shearing. In tension, shear bands at the sample surface make an angle of about 45° with the loading direction. During bending, on the other hand, shear bands appear at the surface perpendicular to the major strain, but the direction of propagation towards the thickness is inclined 45°. The main micromechanisms that lead to damage are interface decohesion, resulting from a strain gradient at the interface, and cracking of martensite. Damage and fracture are delayed in the QP980 steel due to its microstructural constituents' better mechanical compatibility and the transformation-induced plasticity's effect in suppressing damage.

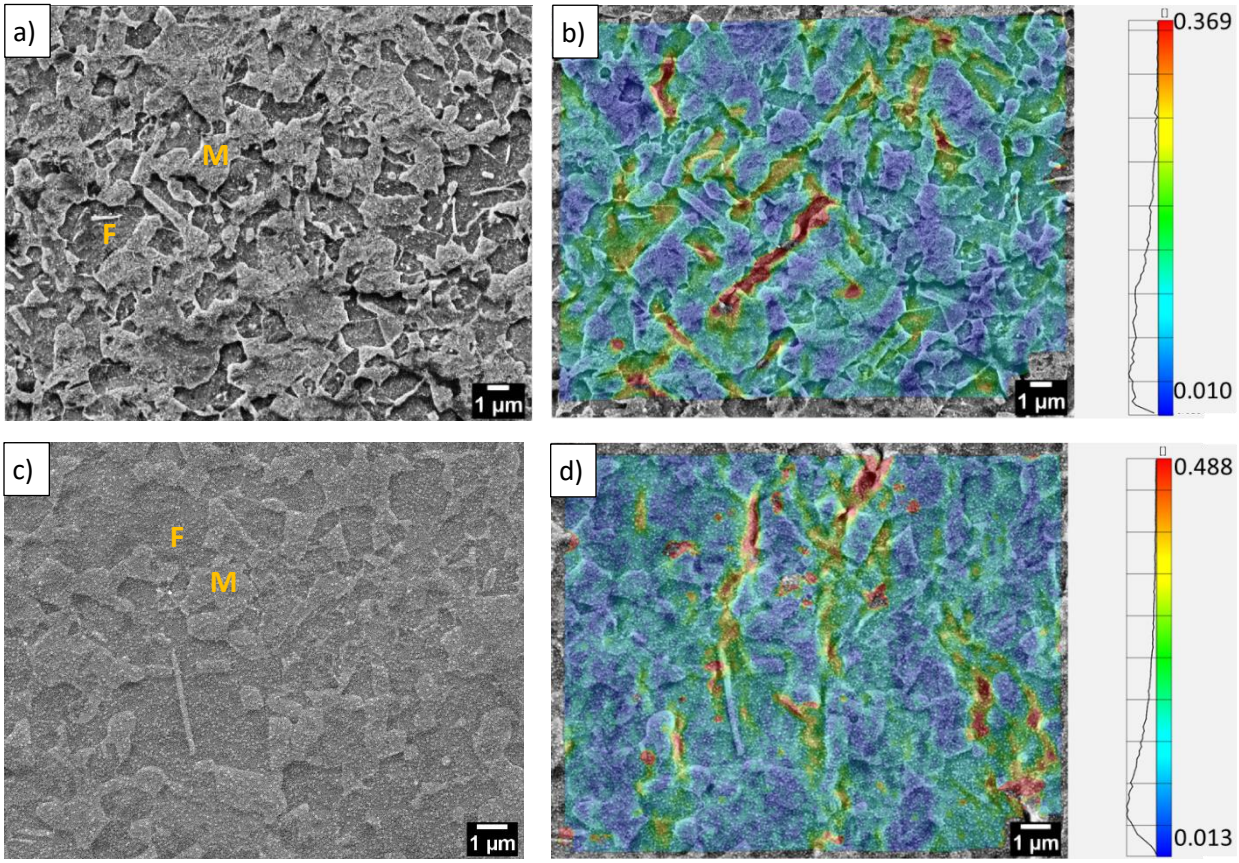

Fig.1 – Microstructure and strain distribution map of the DP980 steel during in situ SEM tensile and bend testing. a) Undeformed microstructure of the tensile sample. b) Von-Mises strain map superimposed on the tensile sample microstructure at an average local strain of 0.11. c) Undeformed microstructure of the bending sample. d) Von-Mises strain map superimposed on the bending sample microstructure at an average local strain of 0.14. F denotes ferrite, and M is martensite.

Acknowledgements
We acknowledge the support of the Natural Sciences and Engineering Research Council of Canada (NSERC). The authors would also like to thank Jeff Gao and Brian Nelson at ArcelorMittal Dofasco, Hamilton, ON, Canada, for providing the material used in this study.

References
[1] B. M. Hance, *SAE Int. J. Mater. Manuf.*, 2018, pp. 505-516.
[2] J. Samei, C. Pelligra, M. Amirmaleki, and D. S. Wilkinson, *Mater. Lett.*, 2020, p. 127664.
[3] D. Yan, C. C. Tasan, and D. Raabe, *Acta Mater.*, 2015, pp. 399-409.
[4] F. Abu-Farha *et al.*, *Metall. Mater. Trans. A*, 2018, pp. 2583-2596.
[5] C. Pelligra, J. Samei, J. Kang, and D. S. Wilkinson, *Int. J. Plast.*, 2022 p. 103435.
[6] D. Frómeta *et al.*, *Metall. Mater. Trans. A*, 2021, pp. 840-856.